

Transferable Relativistic Predictor: Mitigating Cross-Task Cold-Start Issue in NAS

Nan Li^{1,2}, Bing Xue^{2,3}, Lianbo Ma^{1*} and Mengjie Zhang^{2,3}

¹College of Software, Northeastern University

²Centre for Data Science and Artificial Intelligence

³School of Engineering and Computer Science, Victoria University of Wellington
2010500@stu.neu.edu.cn, malb@swc.neu.edu.cn, {bing.xue, mengjie.zhang}@ecs.vuw.ac.nz

Abstract

In neural architecture search (NAS), the relativistic predictor has recently emerged as an attractive technique to solve ranking issue for performance evaluation by predicting the relativistic ranking of architecture pair rather than the absolute performance of an architecture. However, it suffers from a significant cold-start issue, requiring a large amount of evaluated architectures to train an effective predictor on new datasets. In this paper, we propose a transferable relativistic predictor (TRP). Specifically, we construct a proxy dataset using the transferable cheaper-to-obtain performance estimation to softly label the rank between architectural pairs. The soft label with a smooth and easy-to-optimize loss function facilitates the learning of expressive and generalizable representations on the proxy dataset. Furthermore, we construct Chebyshev interpolation for correlation curve to adaptively determine the number of evaluated architectures required on each dataset. Extensive experimental results in different search spaces show the superior performance of TRP compared with state-of-the-art predictors. TRP requires only 54 and 73 evaluated architectures for a warm start on the CIFAR-10 and CIFAR-100 under the DARTS search space.

1 Introduction

Neural architecture search (NAS) [Elsken *et al.*, 2019] has successfully emerged in automatically constructing network architectures for various tasks, including image classification [Huang *et al.*, 2024], objective detection [Wang *et al.*, 2020] and semantic segmentation [Zhang *et al.*, 2021a]. Typical NAS frameworks find the best architecture in a vast search space based on a predefined performance metric (e.g., accuracy [Shen *et al.*, 2023]), where training and evaluating candidate architectures requires substantial computational resources, limiting NAS applications in real-world scenarios [Huang *et al.*, 2024]. To alleviate this issue, various methods are developed to reduce the overheads of architecture evaluations, such as predictor [Wen *et al.*, 2020], parameter sharing

[Shen *et al.*, 2023], and zero-shot metric [Mellor *et al.*, 2021].

Many predictor-based NAS methods sample a set of evaluated architectures to train an accuracy predictor [Ma *et al.*, 2024], aiming to learn the mapping relationship between architecture encodings and their corresponding absolute performance [Wen *et al.*, 2020]. However, these predictors often face ranking issue caused by prediction biases, i.e., architectures with similar performance may be inaccurately ranked during the architecture search process, leading to suboptimal performance [Huang *et al.*, 2022].

Recently, relativistic predictor focuses on comparing the relativistic performance of paired architectures rather than predicting their absolute performances, effectively mitigating the ranking issue [Huang *et al.*, 2022; Xu *et al.*, 2021]. However, such predictors still face cold-start issue: *When applied to new datasets, the effective relativistic predictor needs to be trained from scratch by a large number of evaluated architectures for constructing the relativistic dataset, which remains a computationally expensive process* [Zhao *et al.*, 2023].

Typical relativistic predictors use accuracy to label architectural superior-inferior relationship. This paper exploits transferable relativistic label from the cheaper-to-obtain performance estimation (i.e., zero-shot metric), which can roughly label the relativistic superiority or inferiority between architecture pairs on a proxy dataset for pretraining relativistic predictor. Learning to fit transferable relativistic label may encourage predictor to extract better ranking ability in advance, thereby facilitating a warm start on new datasets. In other words, a pretrained predictor with good ranking ability requires only a small number of evaluated architectures to achieve excellent predictive results on the new datasets. A straightforward approach is to pretrain the predictor by utilizing relativistic label of a single zero-shot metric on the proxy dataset and then finetune it on a small number of evaluated architectures from the new dataset. Table 1 presents preliminary experiments, yielding following observations.

1) Transferable relativistic label can significantly enhance ranking performance. For example, using NWOT [Mellor *et al.*, 2021] increases Kendall’s Tau by 0.3811 and 0.5062 on Ninapro and SCIFAR100, respectively.

2) Inappropriate use of transferable relativistic label may degrade ranking performance. For instance, using JACOV [Mellor *et al.*, 2021] decreases Kendall’s Tau by 0.01 and 0.0053 on ImageNet16-120 and Ninapro, respectively.

*Corresponding author.

Zero-shot	Pretrained Correlation/Finetuning Correlation					
	CIFAR10	CIFAR100	ImageNet16-120	Ninapro	SVHN	SCIFAR100
NWOT	0.2558/0.5459 ↑	0.4901/0.5002 ↑	0.6331/0.6421 ↑	0.3851/0.7627 ↑	0.5555/0.5434 ↓	0.2711/0.7773 ↑
SYNFLOW	0.5536/0.5665 ↑	0.5959/0.6096 ↑	0.3935/0.3951 ↑	0.3554/0.6740 ↑	0.1866/0.3890 ↑	0.6445/0.6383 ↓
SNIP	0.3026/0.5059 ↑	0.4379/0.4436 ↑	0.2759/0.6189 ↑	0.3757/0.7955 ↑	0.3563/0.3878 ↑	0.3329/0.5935 ↑
JACOV	0.3981/0.4012 ↑	0.5527/0.6394 ↑	0.7248/0.7148 ↓	0.4688/0.4635 ↓	0.3092/0.3797 ↑	0.3886/0.5682 ↑

Table 1: Pretrained and finetuning ranking correlations obtained by utilizing different typical types of relativistic label. Specifically, the relativistic label of CIFAR10 is used as the proxy dataset for pretraining the predictor. The pretrained model is subsequently evaluated not only on CIFAR10 itself but also on other target datasets (i.e., CIFAR100, ImageNet16-120, Ninapro, SVHN, and SCIFAR100) to assess its cross-dataset performance before finetuning. After finetuning on each target dataset, the correlations are re-evaluated to measure the performance improvement. All correlations use Kendall’s Tau metric, where the first and second values of each data mean Kendall’s Tau for the pretrained model and Kendall’s Tau for the finetuned model, respectively.

3) Different datasets exhibit varied preferences for transferable relativistic label. For example, SYNFLOW [Tanaka *et al.*, 2020] reduces Kendall’s Tau on SCIFAR100 but enhances predictions on other datasets.

4) Relativistic label is generally positively transferable across most datasets. For instance, NWOT, SYNFLOW, SNIP [Lee *et al.*, 2018], and JACOV show positive transferability in 5, 5, 6, and 4 datasets, respectively.

Preliminary experiments demonstrate that transferable relativistic label improves ranking ability with limited evaluated architectures. This indicates that transferable relativistic label can effectively mitigate the cold-start issue. However, such a naive approach, which highly relies on selection of which single zero-shot metric, fails to fully exploit complementary knowledge from different zero-shot metrics. Therefore, integrating multiple metrics can better mitigate cold-start issue.

Accordingly, this paper proposes a transferable relativistic predictor (TRP). The proposed predictor comprises two steps. During the pretraining stage, we employ the proposed loss function, characterized by its smoothness and ease of optimization, to improve ranking ability on the relativistic dataset, which is softly labeled using multiple zero-shot metrics. During the finetuning stage, we approximate the ranking correlation function of TRP using Chebyshev interpolation. A point where the marginal benefit is less than a certain threshold value indicates the number of evaluated architectures required to finetune TRP on the target dataset. This method can adaptively determine the number of evaluated architectures. The contributions can be summarized as follows.

1) We propose a transferable relativistic predictor (TRP), which can effectively mitigate the cold-start issue by full use of the transferable relativistic label from multiple zero-shot metrics.

2) We provide theoretical analyses of the designed loss function from Bayes consistency and risk minimization, demonstrating its advantages in obtaining better ranking representation.

3) We run extensive experiments. Specifically, the number of evaluated architectures needed by TRP is fewer than that of most existing predictors. TRP can achieve good results in NAS-Bench-201, TransferNAS-Bench101-Micro, TransferNAS-Bench101-Macro, and DARTS search spaces.

2 Related Works

Zero-shot metrics. These metrics eliminate the need for architecture training and can quickly quantify the performance

of architectures by the theoretical-based and empirical-based methods [Chen *et al.*, 2024]. Typically, such metrics require less than one second for architectural evaluation [Chen *et al.*, 2021a]. In addition, numerous studies [Krishnakumar *et al.*, 2022; Chen *et al.*, 2024; Li *et al.*, 2024] have observed that some training-free metrics (e.g., NWOT [Mellor *et al.*, 2021] and FLOPS [Ning *et al.*, 2021]) obtain better ranking correlations on different datasets with the same search space. However, there is no zero-shot metric that achieves good ranking quality in all search spaces, and the optimal zero-shot metric varies from search space [Ning *et al.*, 2021].

Predictor-based NAS. The accuracy predictor has achieved remarkable success in performance evaluation, but expensive evaluated architectures still limit the development. Early works have attempted to fully exploit the limited evaluated architectures to improve accuracy predictor performance from the perspective of operation hierarchy [Chen *et al.*, 2021c], spatial topology information [Lu *et al.*, 2021a], and information flow [Ning *et al.*, 2020], respectively. In addition, some works convert learning methods from supervised learning to semi-supervised learning [Luo *et al.*, 2020; Liu *et al.*, 2021] and self-supervised learning [Ji *et al.*, 2024; Wei *et al.*, 2021; Zheng *et al.*, 2024], alleviating the need for evaluated architectures. However, the accuracy predictor with poor ranking correlation between ground-truth performance and the predicted performance can mislead the search algorithm leading to the selection of a low-ranking architecture.

To tackle this, the relativistic predictor is designed to learn the relativistic ranking of architectures rather than their absolute performances [Huang *et al.*, 2022; Hu *et al.*, 2021; Guo *et al.*, 2024; Chen *et al.*, 2021b]. Among these, NARQ2T [Guo *et al.*, 2024] acquires knowledge of the performance distributions within the search space, facilitating the generalization of its ranking ability across datasets. Arch-Graph [Huang *et al.*, 2022] generalizes task embedding to predict relativistic relation between architecture pairs. Although NARQ2T and Arch-Graph achieve cross-dataset generalization, they still demand substantial evaluated architectures during training. In addition, these works use the hinge function, which is non-smooth and difficult to optimize/learn the relativistic relationship between architecture pairs, leading to poor ranking ability.

Zero-shot metrics in predictor-based NAS. Recent studies have attempted to exploit zero-shot metrics for achieving better search efficiency. For example, the work [White *et al.*, 2021b] finds that certain zero-shot metrics can improve the

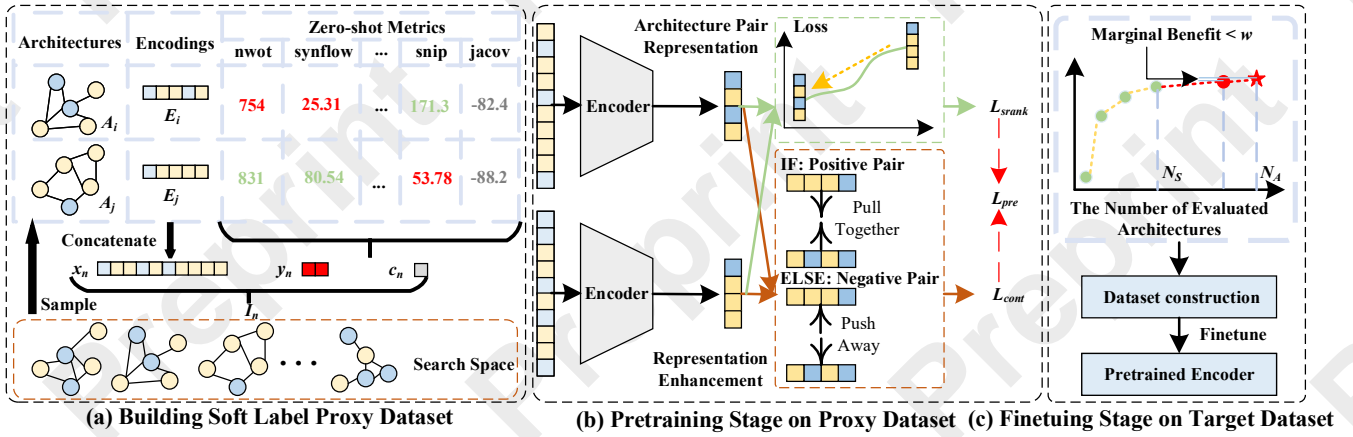


Figure 1: The overall framework of the proposed TRP method consists of three stages: (a) **Building Soft Label Proxy Dataset**: Large-scale architecture pairs are assigned soft labels derived from relativistic label across multiple zero-shot metrics. (b) **Pretraining Stage on Proxy Dataset**: A carefully designed loss function, combining smoothness and ease of optimization with a contrastive learning approach, is used to extract architecture pair representations. (c) **Finetuning Stage on Target Dataset**: An interpolation strategy determines the required quantity of evaluated architectures for finetuning the predictor.

predictive power of the accuracy predictor. ProxyBO [Shen *et al.*, 2023] proposes to combine the architecture ranking given by the accuracy predictor and zero-shot metrics in the search process. AceNAS [Zhang *et al.*, 2021b] pretrains the accuracy predictor based on FLOPS and #PARAMS. DELE [Zhao *et al.*, 2023] dynamically integrates zero-shot metrics for pre-training accuracy predictor. However, such predictors are still subject to the ranking issue.

3 Methodology

As shown in Figure 1, the overall framework of the proposed TRP method contains three parts, i.e., building soft label proxy dataset, pretraining stage on proxy dataset, and finetuning stage on target dataset.

3.1 Building Soft Label Proxy Dataset

Given a search space, two architectures A_i and A_j are randomly sampled to construct an instance I_n for proxy dataset D_P . The encodings E_i and E_j corresponding to A_i and A_j are concatenated to form the input feature x_n . Considering the imprecision of zero-shot metrics (especially when the values of the metrics for the two architectures are close [Mellor *et al.*, 2021]), soft label y_n and confidence score c_n are used to measure relativistic knowledge from K zero-shot metrics at a fine-grained level. y_n is a two-dimensional vector, where the first dimension y_n^1 denotes the probability that A_i is significantly better than A_j , and the second dimension y_n^2 denotes the probability that A_j is significantly better than A_i . We first judge whether A_i or A_j is significantly superior or inferior than the other based on Eq. (1).

$$\rho = \frac{|M_{A_i} - M_{A_j}|}{\max(M_{A_i}, M_{A_j})}, \quad (1)$$

where M_{A_i} and M_{A_j} are the metric values of architectures A_i and A_j , respectively. The selection of ρ is decided by experiment instead of a statistical significance test. If ρ is greater than threshold, there is a significant superior-inferior

relationship between A_i and A_j . Conversely, there is no significant superior-inferior relationship. N_i , N_j , and N_{ij} indicate the number of metrics where A_i is significantly better than A_j , A_j is significantly better than A_i , and neither is significantly better, respectively. Based on this, y_n^1 and y_n^2 are equal to N_i/K and N_j/K , respectively. For confidence score c_{ij} , the smaller N_{ij} indicates that the annotation is more reliable. Thus, c_n is equal to $1 - (N_{ij}/K)$. Repeating the above process N times, we can obtain the proxy dataset D_P . Due to the architecture pair with transferable relativistic label, the pretrained predictor on D_P can obtain better representations.

3.2 Pretraining Stage on Proxy Dataset

For architectural pair representation, the normal ranking loss can be defined as Eq. (2) [Xu *et al.*, 2021; Guo *et al.*, 2024].

$$\mathcal{L}_{rank} = \sum_{n=1}^N \psi(f(x_n)) * \text{sign}(y_n^1 - y_n^2), \quad (2)$$

where $\psi(\cdot)$ is a hinge function with a hyperparameter α , which is usually set to 1 to control the margin (see Eq. (3)). Unfortunately, the hinge function is non-smooth and thus is difficult to optimize for better ranking ability.

$$\psi(f(x_n)) = \max(0, \alpha + f_1(x_n) - f_0(x_n)), \quad (3)$$

where $f_1(x_n)$ and $f_0(x_n)$ are the predicted values of x_n , respectively. Given proxy dataset D_P , we develop a smooth approximation of Eq. (2) via the log-sum-exp function,

$$\mathcal{L}_{rank} = \log \left(1 + \sum_{n=1}^N c_n * \exp((f_1(x_n) - f_0(x_n)) * \text{sign}(y_n^1 - y_n^2)) \right). \quad (4)$$

\mathcal{L}_{rank} form is, asymptotically, an upper bound of the following hinge loss form,

$$\mathcal{L}_{sr\text{rank}}^{\text{asym}} = \sum_{n=1}^N c_n * \psi^*((x_n)) * \text{sign}(y_n^1 - y_n^2), \quad (5)$$

where

$$\psi^*((f(x_n))) = c_n * \max(0, \alpha^* + f_1(x_n) - f_0(x_n)), \quad (6)$$

which allows the predictor to have adaptive margins α^* per architecture pair. It is differentiable and smooth everywhere, which makes it easier to optimize for obtaining better ranking ability. We give theoretical analysis of $\mathcal{L}_{sr\text{rank}}$ in Section 4.

To enhance the architecture pair representations, we employ contrastive learning [Xiao *et al.*, 2024] to maximize similarity among positive data while ensuring dissimilarity for negative samples, thereby aligning architecture pair representations for semantically similar data. Our approach treats different instances with the same soft label as positive data and instances with the different soft label as negative data. We calculate the representation similarity of two instances x_i and x_j , where the embeddings are obtained with an encoder $z(\cdot)$:

$$s(x_i, x_j) = \frac{z(x_i) * z(x_j)}{\|z(x_i)\| * \|z(x_j)\|}. \quad (7)$$

The contrastive learning requires similar data to yield a larger $s(\cdot)$. The contrastive loss is as follows:

$$\mathcal{L}_{cont} = - \sum_{n=1}^N \log \frac{\exp(s(x_n, k_+)/\tau)}{s(x_n, k_+)/\tau + \sum_{i=1}^N \exp(s(x_n, k_-)/\tau)}, \quad (8)$$

where τ is a temperature hyperparameter. k_+ and k_- denote positive and negative data, respectively. The final loss function is the combination of Eqs. 4 and 8.

$$\mathcal{L}_{pre} = \mathcal{L}_{sr\text{rank}} + \lambda_1 \mathcal{L}_{cont}, \quad (9)$$

where λ_1 is a hyperparameter to control the importance between two different loss functions. Therefore, the proposed loss function has a twofold effect. The first is to maximize the capture of relativistic knowledge in soft labels through a smooth and easy-to-optimize loss function (i.e., $\mathcal{L}_{sr\text{rank}}$). The second is the acquisition of more discriminative ranking representations through contrastive loss (i.e., \mathcal{L}_{cont}).

3.3 Finetuning Stage on Target Dataset

After pretraining stage, finetuning is required to transfer the pretrained predictor to the target task. However, how to choose the appropriate number of evaluated architectures still requires trial and error. To solve the issue, we design an interpolation-based method to select the number of evaluated architectures adaptively. Specifically, we first sample a small number of evaluated architectures (N_s) from the target dataset. Interpolated data points are denoted as $D_I = (m_i, r_i)$, where r_i refers to Kendall's Tau correlation for N_s evaluated architectures after finetuning via m_i samples. Based on D_I , we fit a curve of the relationship between the number of evaluated architectures and Kendall's Tau correlation by

Chebyshev interpolation polynomial (i.e., Eq. (10)) [Rivlin, 2020].

$$P(m) = \sum_{i=0}^{N_s} r_i \prod_{\substack{j=0 \\ j \neq i}}^{N_s} \frac{m - m_j}{m_i - m_j}. \quad (10)$$

The marginal benefit is the first order derivative of Eq. (10) as follows:

$$P'(m) = \sum_{i=0}^{N_s} r_i \frac{d}{dm} \left[\prod_{\substack{j=0 \\ j \neq i}}^{N_s} \frac{m - m_j}{m_i - m_j} \right]. \quad (11)$$

The optimal number of evaluated architectures is $N_A = \min \{m \in \mathbb{N} \mid P'(x) \leq \omega\}$. The relativistic dataset D_T with size $2N_A(N_A-1)$ is constructed to finetune the predictor. Unlike D_P , labels in D_T are based on ground-truth performances of architecture pairs. If A_i is better than A_j , y_n^1 and y_n^2 are 1 and 0, respectively. Otherwise, y_n^1 and y_n^2 are 0 and 1. Furthermore, D_T is without confidence score. The following loss function is used in finetuning stage,

$$\mathcal{L}_{fine} = \mathcal{L}_{sr\text{rank}}^* + \lambda_2 \mathcal{L}_{cont}, \quad (12)$$

where λ_2 is to control the importance between two different loss functions. $\mathcal{L}_{sr\text{rank}}^*$ is version of Eq. (4) without confidence score c_n .

4 Theoretical Analysis

We prove the benefit of Eq. (4) from the point of view of Bayes consistency and risk minimization. Bayes consistency is a critical attribute of loss function for achieving the right objective [Saberian and Vasconcelos, 2011]. The output of the predictor is a two-dimensional vector $[f_F(x), f_L(x)]$, where $f_F(x)$ and $f_L(x)$ are the superiority and inferiority scores in architectural pairs, respectively. Based on Bayes prediction rule, we can obtain the followings:

$$f^*(x) = \arg \max_{y \in \mathcal{Y}} P(Y = y \mid x), \quad (13)$$

where $\mathcal{Y} \in \{F, L\}$ is the label space. F and L denote the labels in architectural pairs in which the former is superior to the latter and the latter is better than the former, respectively. The outputs to the predictor need to be satisfied:

$$f_F(x) - f_L(x) = \log \frac{P(Y = F \mid x)}{P(Y = L \mid x)}. \quad (14)$$

Due to $\Delta f(x_n) = f_1(x_n) - f_0(x_n)$, when $\text{sign}(y_n^1 - y_n^2) = 1$, $\exp((f_1(x_n) - f_0(x_n)) * \text{sign}(y_n^1 - y_n^2)) = \exp(\Delta f(x_n))$. When $\text{sign}(y_n^1 - y_n^2) = 0$, $\exp((f_1(x_n) - f_0(x_n)) * \text{sign}(y_n^1 - y_n^2)) = \exp(-\Delta f(x_n))$. Thus, Eq. (4) = $\log \left(1 + \sum_{n=1}^N c_n * \exp(\pm \Delta f(x_n)) \right) \approx \sum_{n=1}^N c_n * \exp(-\frac{1}{2} \Delta f(x_n))$.

Considering the loss of a single architecture pair, since c_n as a real number cannot affect the subsequent proof, $\mathcal{L}_{sr\text{rank}}$ in Eq. (4) loss is analytically equivalent to the following loss without the logarithmic,

$$\ell_{\text{rank}}(f(x), Y) = \exp\left(-\frac{1}{2}\Delta f(x)\right), \quad (15)$$

where $\Delta f(x) = f_F(x) - f_L(x)$. When $\Delta f(x) \gg 0$, i.e., $f_F(x) \gg f_L(x)$, it indicates that score of F is significantly higher than L , and loss approaches zero. The loss function drives predictor training, making $\Delta f(x)$ increasingly larger, aligning predictor’s predictions with Bayes consistency.

Proof. Consider $f(x)$ that minimizes the risk, The total risk function of the predictor is defined as:

$$R(f) = \mathbb{E}_{(x,Y) \sim \mathcal{D}} [\ell_{\text{rank}}(f(x), Y)]. \quad (16)$$

The conditional risk function is defined as:

$$R(f | x) = \mathbb{E}_{Y \sim P(Y|x)} [\ell_{\text{rank}}(f(x), Y)]. \quad (17)$$

Substituting the loss function, we have:

$$R(f | x) = P(Y = F | x) \exp\left(-\frac{1}{2}\Delta f(x)\right) + P(Y = L | x) \exp\left(\frac{1}{2}\Delta f(x)\right). \quad (18)$$

The first and second order derivatives of Eq. (18) are

$$\frac{\partial R(f | x)}{\partial \Delta f(x)} = -\frac{1}{2}P(Y = F | x) \exp\left(-\frac{1}{2}\Delta f(x)\right) + \frac{1}{2}P(Y = L | x) \exp\left(\frac{1}{2}\Delta f(x)\right) \quad (19)$$

$$\frac{\partial^2 R(f | x)}{\partial \Delta f(x)^2} = \frac{1}{4}P(Y = F | x) \exp\left(-\frac{1}{2}\Delta f(x)\right) + \frac{1}{4}P(Y = L | x) \exp\left(\frac{1}{2}\Delta f(x)\right) \quad (20)$$

Since $P(Y = F | x)$ and $P(Y = L | x)$ are non-negative, and the exponential function is always greater than zero, the second-order derivative is always positive, indicating that the risk function is convex and exists a global minimum solution. Making the first order derivative equal to 0 obtains the minimum value of the risk function $\Delta f(x) = \log \frac{P(Y=F|x)}{P(Y=L|x)}$ consistent with the predictor’s output. $f^*(x)$ implements the Bayes prediction rule in Eq. (13). Thus, we can say that using Eq. (4) achieves the right objective and extracts better architecture pair representations for predictor.

5 Experiments and Results

The experiments contain ranking capability, search results, and ablation studies. We run experiments on three closed domain search spaces and one open domain search space.

Method	CIFAR-10		CIFAR-100		ImageNet16-120	
	Query	τ	Query	τ	Query	τ
CAP †	50	0.5733	50	0.5663	50	0.5697
DCLP †	50	0.6090	50	0.5899	50	0.5828
DELE †	45	0.6447	45	0.6427	45	0.6328
Arch-Graph †	150	0.6724	150	0.6674	150	0.6533
ReNAS †	90	0.6529	90	0.6411	90	0.6458
TRP (Ours)	30	0.8324	34	0.8267	41	0.8286

Table 2: Ranking results on NAS-Bench-201. Kendall’s Tau (τ) of 10 independent runs is calculated. †: implemented by ourselves using open source code. The **best** and **second best** are color coded.

5.1 Results on NAS Benchmarks

The experiments are conducted on NAS-Bench-201 and TransNAS-Bench-101 benchmarks. Kendall’s Tau is used to evaluate the predictor’s ranking capability, while a query metric represents the amount of evaluated architectures required by the predictor. TRP focuses on the relative relationship between two architectures, and an additional bubble sort is necessary to determine the predicted ranking for a set of architectures, where TRP is used to decide whether to swap the rankings of two architectures. The closer Kendall’s Tau value is to 1, the higher the agreement between actual accuracy ranking and predicted ranking, indicating the better ranking capability of TRP. For the query metric, we adopt experimental results from the original literature. If the predictor has not been tested on a NAS benchmark, default settings from the source code are applied. In NAS-Bench-201, the proxy dataset is constructed using zero-shot metrics on CIFAR-10 for pre-training, followed by finetuning on CIFAR-10, CIFAR-100, and ImageNet16-120. For TransNAS-Bench-101, zero-shot metrics from the objective classification task are used to construct the proxy dataset, and finetuning is performed on all datasets. The number of queries is adaptively determined using the proposed interpolation method.

The ranking results on NAS-Bench-201 are recorded in Table 2. Compared with existing pretraining-finetuning accuracy predictors (i.e., CAP, DCLP, and DELE) and relativistic predictors (Arch-Graph and ReNAS), TRP achieves the best Kendall’s Tau on the three datasets with the fewest number of evaluated architectures (CIFAR-10: 30, CIFAR-100: 34 and ImageNet16-120: 41). Notably, with only 30 evaluated architectures (1/3 of Arch-Graph), Kendall’s Tau of TRP achieves 0.1805 improvement on the CIFAR-10. Moreover, we report the ranking results on TransNAS-Bench-101 in Table 3. It can be observed that TRP obtains state-of-the-art performance when compared with other competitors regardless of the datasets. Moreover, it is noteworthy that TRP surpasses the second-best predictors (i.e., DELE and ReNAS) by at least 0.22 Kendall’s Tau on all tasks in the macro and micro search spaces. Compared to Arch-Graph (50), which is also tested on TransNAS-Bench-101, we are at least 10 the evaluated architectures fewer than Arch-Graph is, but obtain an improvement of at least 0.25 Kendall’s Tau.

Such good results imply that the pretraining stage can fully utilize the transferable relativistic label from zero-shot metrics via the designed soft label and loss function. The pre-trained predictor can learn meaningful architecture pair representations for the architectural pairs even before the fine-

Search Space	Method	Cls. Obj.		Cls. Scene		Auto.		Normal		Sem. Seg.		Room.		Jigsaw	
		Query	τ	Query	τ	Query	τ	Query	τ	Query	τ	Query	τ	Query	τ
Micro	CAP†	50	0.5648	50	0.5557	50	0.557	50	0.5619	50	0.5582	50	0.5524	50	0.5596
	DCLP†	50	0.6075	50	0.5977	50	0.6089	50	0.6105	50	0.6081	50	0.5902	50	0.6083
	DELE†	45	0.6306	45	0.6339	45	0.6369	45	0.6304	45	0.6261	45	0.6275	45	0.6327
	Arch-Graph†	50	0.6063	50	0.5918	50	0.6021	50	0.6069	50	0.5906	50	0.6084	50	0.6023
	ReNAS†	90	0.6378	90	0.6277	90	0.6297	90	0.6377	90	0.6319	90	0.6233	90	0.6269
	TRP (Ours)	31	0.8584	28	0.8620	33	0.8771	34	0.8695	29	0.8697	40	0.8709	38	0.8513
Macro	CAP†	50	0.5545	50	0.5594	50	0.5553	50	0.5586	50	0.5583	50	0.5572	50	0.5672
	DCLP†	50	0.6011	50	0.5963	50	0.6034	50	0.5920	50	0.5978	50	0.6101	50	0.5995
	DELE†	45	0.6295	45	0.6238	45	0.6357	45	0.6379	45	0.6246	45	0.6327	45	0.6418
	Arch-Graph†	50	0.6004	50	0.6040	50	0.5942	50	0.5989	50	0.6029	50	0.6009	50	0.6073
	ReNAS†	90	0.6251	90	0.6281	90	0.6342	90	0.6250	90	0.6392	90	0.6324	90	0.6325
	TRP (Ours)	33	0.8551	36	0.8503	34	0.8715	37	0.8527	33	0.8667	39	0.8515	37	0.8609

Table 3: Ranking results on TransNAS-Bench-101. The Kendall’s Tau (τ) of 10 independent runs is calculated. †: implemented by ourselves using open source code. The best and second-best are color coded.

Method	CIFAR-10		CIFAR-100		ImageNet16-120		Search Cost (Seconds) ↓
	Val. Acc (%) ↑	Test. Acc (%) ↑	Val. Acc (%) ↑	Test. Acc (%) ↑	Val. Acc (%) ↑	Test. Acc (%) ↑	
ResNet [2016]	90.83	93.97	70.42	70.86	44.53	43.63	–
ENAS [2018]	37.51 ± 3.19	53.89 ± 0.58	13.37 ± 2.35	13.96 ± 2.33	15.06 ± 1.95	14.84 ± 2.10	13314.51
DARTS [2018b]	39.77 ± 0.00	54.30 ± 0.00	15.03 ± 0.00	15.61 ± 0.00	16.43 ± 0.00	16.32 ± 0.00	10889.87
Arch2Vec-BO [2020]	91.41 ± 0.22	94.18 ± 0.24	73.35 ± 0.32	73.37 ± 0.30	46.34 ± 0.18	46.27 ± 0.37	12000
RMI-NAS [2022]	91.44 ± 0.09	94.28 ± 0.10	73.38 ± 0.14	73.36 ± 0.19	46.37 ± 0.00	46.34 ± 0.00	1258.21
CAP [2024]	91.54 ± 0.10	94.34 ± 0.06	73.41 ± 0.17	73.41 ± 0.22	46.47 ± 0.07	46.44 ± 0.36	15.65
ReNAS [2021]	90.90 ± 0.31	93.99 ± 0.25	71.96 ± 0.99	72.12 ± 0.79	45.85 ± 0.47	45.97 ± 0.49	86.31
LCMNAS [2023]	91.22 ± 0.17	94.05 ± 0.07	71.96 ± 0.96	72.01 ± 0.82	45.55 ± 0.78	45.61 ± 0.08	11521
BOHB [2018]	90.82 ± 0.53	93.61 ± 0.52	70.74 ± 1.29	70.85 ± 1.28	44.26 ± 1.36	44.42 ± 1.49	12000
Jacob cov [2021]	89.69 ± 0.73	92.96 ± 0.80	69.87 ± 1.22	70.03 ± 1.16	43.99 ± 2.05	44.43 ± 2.07	–
SETN [2019a]	82.25 ± 5.17	86.19 ± 4.63	56.86 ± 7.59	56.87 ± 7.77	32.54 ± 3.63	31.90 ± 4.07	31009.81
ParZC [2024]	91.55 ± 0.02	94.36 ± 0.25	73.49 ± 0.02	73.31 ± 0.02	46.37 ± 0.04	46.34 ± 0.01	68.95
GDAS [2019b]	90.00 ± 0.21	93.51 ± 0.13	71.14 ± 0.27	70.61 ± 0.26	41.70 ± 1.26	41.84 ± 0.90	28926
TRP	91.57 ± 0.01	94.36 ± 0.15	73.49 ± 0.01	73.44 ± 0.02	46.49 ± 0.05	46.48 ± 0.27	14.97
Optimal	91.61	94.37	73.49	73.51	46.73	47.31	–

Table 4: Comparison with the SOTA methods on NAS-Bench-201. The best and second-best are color coded.

tuning stage. Thus, only a few evaluated architectures are enough for a warm start of the predictor on new datasets.

5.2 Searching on Closed Domain Search Spaces

On NAS-Bench-201, the total number of queried architectures is determined by an interpolation-based method (see Table 2). We follow the settings in [Dong and Yang, 2020] to search for architectures. Specifically, the predictor evaluates all architectures in the search space. The best performance of the first 50 evaluated architectures is reported as the search result (see Table 4). Compared with competitors, TRP completes the evaluation of all architectures using only 15 seconds. In addition, we achieve the best average accuracy on different datasets. Especially, the number of queried architectures is substantially fewer than the accuracy predictor (e.g., CAP) and relativistic predictor (e.g., ReNAS). For fair comparison on TransNAS-Bench-101, we follow the settings in [Huang *et al.*, 2022] and the search results are shown in Table 5. On macro and micro search spaces, TRP achieves the best search results on all datasets. Compared to Arch-Graph (query = 50), TRP achieves good results by querying a small number of architectures (query range: 29-40).

These extraordinary results can be attributed to the sufficient transferable relativistic label from zero-shot metrics that the predictor learns in advance through the designed soft label and loss function. Moreover, TRP is finetuned on a

small number of evaluated architectures, and obtains excellent state-of-the-art performances on different datasets across multiple search spaces, further verifying the positive effects of using transferable relativistic label. These promising experimental results demonstrate that the transferable relativistic label facilitates reducing the number of evaluated architectures and mitigating cold-start issue on new datasets.

5.3 Searching on Open Domain Search Space

We construct the proxy dataset using the zero-shot metrics on CIFAR-10 for the pretraining predictor, which is finetuned by CIFAR-10 and CIFAR-100. Following [White *et al.*, 2021a], we randomly select a certain number of architectures in the DARTS search space and then train them from scratch to construct the evaluated architectures for the pretraining predictor, where the number of selected architectures is determined by the proposed adaptive approach. For each selected architecture, the epoch number is set to 50 with a batch size 64. As for the search method, we sample 10k architectures at random in the DARTS search space and evaluate them using our trained predictor. After that, we select the architectures with top-5 predicted performance as the search results and re-train them with common DARTS strategies. The experimental results on CIFAR-10 and CIFAR-100 are shown in Table 6.

Compared to predictor-based NAS approaches, the architectures obtained by TRP achieve minimal loss and #Param

Search Space	Algorithm	Cls. Obj. Acc. (%) \uparrow	Cls. Scene Acc. (%) \uparrow	Auto. SSIM (10^{-3}) \uparrow	Normal SSIM (10^{-3}) \uparrow	Sem. Seg. mIoU (%) \uparrow	Room. L2 loss (10^{-3}) \downarrow	Jigsaw Acc. (%) \uparrow
Micro	RS [2012]	45.16	54.41	55.94	56.85	25.21	61.48	94.47
	REA [2019]	45.39	54.62	56.96	57.22	25.52	61.72	88.95
	PPO [2017]	45.19	54.37	55.83	56.9	25.24	66.98	88.95
	BONAS-t [2020]	45.38	54.57	56.18	57.24	25.24	60.93	–
	Arch-Graph-zero [2022]	45.64	54.8	56.61	57.9	25.73	60.21	–
	Arch-Graph[2022]	45.81	54.9	56.58	58.27	25.69	60.08	–
	weakNAS [2021]	45.66	54.72	56.91	57.21	25.90	60.37	94.63
	CATCH [2020]	45.27	54.38	56.13	56.99	25.38	60.7	–
	TRP (Ours)	45.92	54.77	56.99	58.62	25.90	60.01	94.77
	Optimal	46.32	54.94	57.72	59.62	26.27	59.38	95.37
Macro	RS [2012]	46.85	56.5	70.06	60.7	28.37	59.35	96.78
	REA [2019]	47.09	56.57	69.98	60.88	28.87	58.73	96.88
	BONAS [2020]	46.85	56.47	74.45	61.62	28.82	59.39	96.76
	weakNAS [2021]	47.4	56.88	72.54	62.37	29.18	57.86	96.86
	CATCH [2020]	47.29	56.49	70.36	60.85	28.71	59.37	–
	BONAS-t [2020]	47.06	56.86	71.41	61.44	28.76	58.35	–
	Arch-Graph-zero [2022]	47.42	56.78	75.51	63.39	29.17	58.15	–
	Arch-Graph [2022]	47.44	56.98	75.9	64.35	29.19	57.75	–
	TRP (Ours)	47.52	56.99	75.95	64.35	29.20	57.55	96.97
	Optimal	47.96	57.48	76.88	64.35	29.66	56.28	97.02

Table 5: Comparison with the SOTA methods on TransNAS-Bench-101. The **best** and **second-best** are color coded.

Dataset	Algorithm	#Param (MB) \downarrow	Error (%) \downarrow	Search Cost (GPU Days) \downarrow	Query \downarrow
C10	CATE [2021a]	3.5	2.56	3.3	150
	NPENAS-NP [2022]	3.5	2.44	1.8	100
	TNASP [2021b]	3.7	2.52	0.3	1000
	NAR-Former [2023]	3.8	2.48	0.24	100
	DELE [2023]	4.1	2.3	–	300
	DCLP-RL [2024]	–	2.48	0.17	–
	CAP [2024]	3.3	2.42	3.3	100
	PINAT [2023]	3.6	2.42	0.3	1000
	CATES [2020]	4.1	2.58	–	800
	Arch2vec-BO [2020]	3.6	2.48	100	400
	BONAS-D [2020]	3.3	2.43	10	4800
	TRP (Ours)	3.2	2.40	1.4	54
C100	PNAS [2018a]	3.2	17.63	225	1160
	NAO [2018]	10.6	15.67	200	1000
	DELE [2023]	4.1	16.07	–	300
	TRP (Ours)	3.2	14.94	1.7	73

Table 6: Comparison with the SOTA methods on DARTS search space. The **best** and **second-best** are color coded.

on both datasets. Regarding search cost, we outperform most predictors on CIFAR-10, second only to TNASP and PINAT. In terms of loss, the architecture obtained by TRP is less than TNASP and PINAT by 0.12 and 0.02, respectively. Regarding the number of queried architectures, on CIFAR-10 and CIFAR-100, TRP is only 1/4 of DELE. Using such a small number of queried architectures and obtaining good search results reaffirms the advantages of the proposed predictor for mitigating cold-start issue. More detailed experimental settings are reported in the supplementary materials.

5.4 Ablation Study

We conduct ablation studies for the loss function, including hyperparameters (λ_1 and λ_2), hinge/log-sum-exp, and with/without contrastive loss. Based on Figures 2 (a) and (b), λ_1 and λ_2 for pretraining and finetuning stages should be taken as 7 and 6, respectively, achieving good Kendall’s Tau. Figure 2 (c) proves that the log-sum-exp learns a better representation compared to the hinge loss, facilitating the improvement of the ranking ability of the predictor. The contrastive loss can capture better architecture pair representations (see

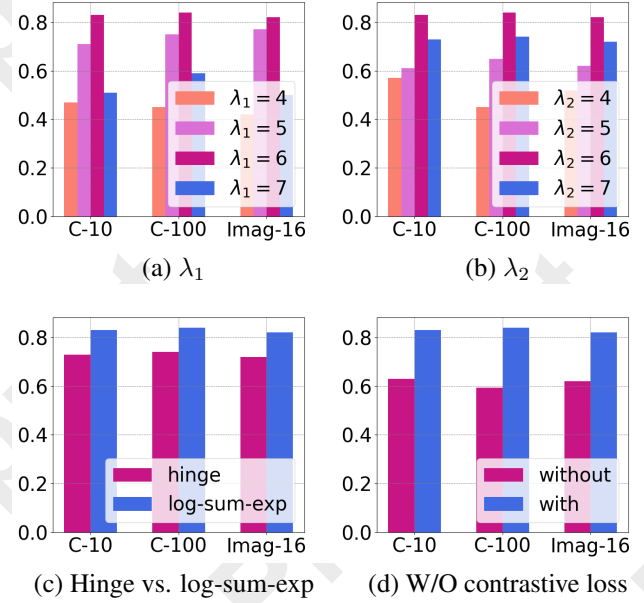


Figure 2: Results of Ablation study for loss function.

Figure 2 (d)). More experiments (e.g., ① **soft label/hard label**, ② **with/without pretraining**, and ③ **finetuning methods**) can be found in the supplementary materials.

6 Conclusions

This paper proposes a transferable relativistic predictor to alleviate cold-start issue. The pretraining stage enhances architecture pair representation with a specialized loss function, and the finetuning stage employs interpolation to determine the amount of evaluated architectures adaptively. Experiments across four search spaces demonstrate that TRP outperforms peer predictor-based NAS methods. We further will explore more information fusion technology to boost in-depth research into the transferable relativistic label.

Acknowledgments

This work is supported in part by the National Natural Science Foundation of China under Grant 62472079, in part by the China Scholarship Council (CSC)/Victoria University Scholarship, and in part by the Special Programme for Doctoral Students under the Young Talent Support Project of CAST.

References

- [Bergstra and Bengio, 2012] James Bergstra and Yoshua Bengio. Random search for hyper-parameter optimization. *JMLR*, 2012.
- [Chen *et al.*, 2020] Xin Chen, Yawen Duan, Zewei Chen, and Hang Xu. Catch: Context-based meta reinforcement learning for transferrable architecture search. In *Proc. of ECCV*, 2020.
- [Chen *et al.*, 2021a] Wuyang Chen, Xinyu Gong, and Zhangyang Wang. Neural architecture search on imagenet in four gpu hours: A theoretically inspired perspective. In *Proc. of ICLR*, 2021.
- [Chen *et al.*, 2021b] Yaofu Chen, Yong Guo, Qi Chen, and Minli Li. Contrastive neural architecture search with neural architecture comparators. In *Proc. of CVPR*, 2021.
- [Chen *et al.*, 2021c] Ziyi Chen, Yibing Zhan, Baosheng Yu, Mingming Gong, and Bo Du. Not all operations contribute equally: Hierarchical operation-adaptive predictor for neural architecture search. In *Proc. of ICCV*, 2021.
- [Chen *et al.*, 2024] Wuyang Chen, Xinyu Gong, Junru Wu, and Yunchao Wei. Understanding and accelerating neural architecture search with training-free and theory-grounded metrics. *IEEE TPAMI*, 2024.
- [Dong and Yang, 2019a] Xuanyi Dong and Yi Yang. One-shot neural architecture search via self-evaluated template network. In *Proc. of CVPR*, 2019.
- [Dong and Yang, 2019b] Xuanyi Dong and Yi Yang. Searching for a robust neural architecture in four gpu hours. In *Proc. of CVPR*, 2019.
- [Dong and Yang, 2020] Xuanyi Dong and Yi Yang. Nas-bench-201: Extending the scope of reproducible neural architecture search. In *Proc. of ICLR*, 2020.
- [Dong *et al.*, 2024] Peijie Dong, Lujun Li, Xinglin Pan, and Zimian Wei. Parzc: Parametric zero-cost proxies for efficient nas. *arXiv preprint arXiv:2402.02105*, 2024.
- [Duan *et al.*, 2021] Yawen Duan, Xin Chen, and Hang Xu. Transnas-bench-101: Improving transferability and generalizability of cross-task neural architecture search. In *Proc. of CVPR*, 2021.
- [Elsken *et al.*, 2019] Thomas Elsken, Jan Hendrik Metzen, and Frank Hutter. Neural architecture search: A survey. *JMLR*, 2019.
- [Falkner *et al.*, 2018] Stefan Falkner, Aaron Klein, and Frank Hutter. Bohb: Robust and efficient hyperparameter optimization at scale. In *Proc. of ICML*, 2018.
- [Guo *et al.*, 2024] Bicheng Guo, Lilin Xu, Tao Chen, and Peng Ye. Latency-aware neural architecture performance predictor with query-to-tier technique. *IEEE TCSVT*, 2024.
- [He *et al.*, 2016] Kaiming He, Xiangyu Zhang, Shaoqing Ren, and Jian Sun. Deep residual learning for image recognition. In *Proc. of CVPR*, 2016.
- [Hu *et al.*, 2021] Chi Hu, Chenglong Wang, Xiangnan Ma, and Xia Meng. Ranknas: Efficient neural architecture search by pairwise ranking. In *Proc. of EMNLP*, 2021.
- [Huang *et al.*, 2022] Minbin Huang, Zhijian Huang, and Changlin Li. Arch-graph: Acyclic architecture relation predictor for task-transferable neural architecture search. In *Proc. of CVPR*, 2022.
- [Huang *et al.*, 2024] Yi-Cheng Huang, Wei-Hua Li, Chih-Han Tsou, Jun-Cheng Chen, and Chu-Song Chen. Upnas: Unified proxy for neural architecture search. In *Proc. of CVPR*, 2024.
- [Ji *et al.*, 2024] Han Ji, Yuqi Feng, and Yanan Sun. Cap: A context-aware neural predictor for nas. In *Proc. of IJCAI*, 2024.
- [Krishnakumar *et al.*, 2022] Arjun Krishnakumar, Colin White, and Arber Zela. Nas-bench-suite-zero: Accelerating research on zero cost proxies. In *Proc. of NeurIPS*, 2022.
- [Lee *et al.*, 2018] Namhoon Lee, Thalaiyasingam Ajanthan, and Philip Torr. Snip: Single-shot network pruning based on connection sensitivity. In *Proc. of ICLR*, 2018.
- [Li *et al.*, 2024] Guihong Li, Duc Hoang, and Kartikeya Bhardwaj. Zero-shot neural architecture search: Challenges, solutions, and opportunities. *IEEE TPAMI*, 2024.
- [Liu *et al.*, 2018a] Chenxi Liu, Barret Zoph, Maxim Neumann, Jonathon Shlens, Wei Hua, Li-Jia Li, Li Fei-Fei, Alan Yuille, Jonathan Huang, and Kevin Murphy. Progressive neural architecture search. In *Proc. of ECCV*, 2018.
- [Liu *et al.*, 2018b] Hanxiao Liu, Karen Simonyan, and Yiming Yang. Darts: Differentiable architecture search. In *Proc. of ICLR*, 2018.
- [Liu *et al.*, 2021] Yuqiao Liu, Yehui Tang, and Yanan Sun. Homogeneous architecture augmentation for neural predictor. In *Proc. of ICCV*, 2021.
- [Lopes and Alexandre, 2023] Vasco Lopes and Luís A Alexandre. Toward less constrained macro-neural architecture search. *IEEE TNNLS*, 2023.
- [Lu *et al.*, 2021a] Shun Lu, Jixiang Li, Jianchao Tan, Sen Yang, and Ji Liu. Tnasp: A transformer-based nas predictor with a self-evolution framework. In *Proc. of NeurIPS*, 2021.
- [Lu *et al.*, 2021b] Shun Lu, Jixiang Li, Jianchao Tan, Sen Yang, and Ji Liu. Tnasp: A transformer-based nas predictor with a self-evolution framework. *Proc. of NeurIPS*, 2021.
- [Lu *et al.*, 2023] Shun Lu, Yu Hu, Peihao Wang, Yan Han, Jianchao Tan, Jixiang Li, Sen Yang, and Ji Liu. Pinat:

- A permutation invariance augmented transformer for nas predictor. In *Proc. of AAAI*, 2023.
- [Luo *et al.*, 2018] Renqian Luo, Fei Tian, Tao Qin, Enhong Chen, and Tie-Yan Liu. Neural architecture optimization. *Proc. of NeurIPS*, 2018.
- [Luo *et al.*, 2020] Renqian Luo, Xu Tan, Rui Wang, Tao Qin, Enhong Chen, and Tie-Yan Liu. Semi-supervised neural architecture search. In *Proc. of NeurIPS*, 2020.
- [Ma *et al.*, 2024] Lianbo Ma, Haidong Kang, Guo Yu, Qing Li, and Qiang He. Single-domain generalized predictor for neural architecture search system. *IEEE TC*, 2024.
- [Mellor *et al.*, 2021] Joe Mellor, Jack Turner, Amos Storkey, and Elliot J Crowley. Neural architecture search without training. In *Proc. of ICML*, 2021.
- [Ning *et al.*, 2020] Xuefei Ning, Yin Zheng, Tianchen Zhao, Yu Wang, and Huazhong Yang. A generic graph-based neural architecture encoding scheme for predictor-based nas. In *Proc. of ECCV*, pages 189–204, 2020.
- [Ning *et al.*, 2021] Xuefei Ning, Changcheng Tang, and Wenshuo Li. Evaluating efficient performance estimators of neural architectures. In *Proc. of NeurIPS*, 2021.
- [Pham *et al.*, 2018] Hieu Pham, Melody Guan, Barret Zoph, Quoc Le, and Jeff Dean. Efficient neural architecture search via parameters sharing. In *Proc. of ICML*, 2018.
- [Real *et al.*, 2019] Esteban Real, Alok Aggarwal, Yanping Huang, and Quoc V Le. Regularized evolution for image classifier architecture search. In *Proc. of AAAI*, 2019.
- [Rivlin, 2020] Theodore J Rivlin. *Chebyshev polynomials*. Courier Dover Publications, 2020.
- [Saberian and Vasconcelos, 2011] Mohammad Saberian and Nuno Vasconcelos. Multiclass boosting: Theory and algorithms. *Proc. of NeurIPS*, 2011.
- [Schulman *et al.*, 2017] John Schulman, Filip Wolski, Prafulla Dhariwal, Alec Radford, and Oleg Klimov. Proximal policy optimization algorithms. *arXiv preprint arXiv:1707.06347*, 2017.
- [Shen *et al.*, 2023] Yu Shen, Yang Li, Jian Zheng, and Wentao Zhang. Proxybo: Accelerating neural architecture search via bayesian optimization with zero-cost proxies. In *Proc. of AAAI*, 2023.
- [Shi *et al.*, 2020] Han Shi, Renjie Pi, Hang Xu, Zhenguo Li, James Kwok, and Tong Zhang. Bridging the gap between sample-based and one-shot neural architecture search with bonas. *Proc. of NeurIPS*, 2020.
- [Tanaka *et al.*, 2020] Hidenori Tanaka, Daniel Kunin, Daniel L Yamins, and Surya Ganguli. Pruning neural networks without any data by iteratively conserving synaptic flow. In *Proc. of NeurIPS*, 2020.
- [Wang *et al.*, 2020] Ning Wang, Yang Gao, and Hao Chen. Nas-fcos: Fast neural architecture search for object detection. In *Proc. of CVPR*, 2020.
- [Wei *et al.*, 2021] Chen Wei, Yiping Tang, and Chuang Niu. Self-supervised representation learning for evolutionary neural architecture search. *IEEE CIM*, 2021.
- [Wei *et al.*, 2022] Chen Wei, Chuang Niu, Yiping Tang, Yue Wang, Haihong Hu, and Jimin Liang. Npenas: Neural predictor guided evolution for neural architecture search. *IEEE TNNLS*, 2022.
- [Wen *et al.*, 2020] Wei Wen, Hanxiao Liu, Yiran Chen, and Hai Li. Neural predictor for neural architecture search. In *Proc. of ECCV*, 2020.
- [White *et al.*, 2021a] Colin White, Willie Neiswanger, and Yash Savani. Bananas: Bayesian optimization with neural architectures for neural architecture search. In *Proc. of AAAI*, 2021.
- [White *et al.*, 2021b] Colin White, Arber Zela, Robin Ru, Yang Liu, and Frank Hutter. How powerful are performance predictors in neural architecture search? *Proc. of NeurIPS*, 2021.
- [Wu *et al.*, 2021] Junru Wu, Xiyang Dai, Dongdong Chen, Yinpeng Chen, Mengchen Liu, Ye Yu, Zhangyang Wang, Zicheng Liu, Mei Chen, and Lu Yuan. Stronger nas with weaker predictors. *Proc. of NeurIPS*, 2021.
- [Xiao *et al.*, 2024] Teng Xiao, Huaisheng Zhu, Zhengyu Chen, and Suhang Wang. Simple and asymmetric graph contrastive learning without augmentations. *Proc. of NeurIPS*, 2024.
- [Xu *et al.*, 2021] Yixing Xu, Yunhe Wang, Kai Han, and Yehui Tang. Renas: Relativistic evaluation of neural architecture search. In *Proc. of CVPR*, 2021.
- [Yan *et al.*, 2020] Shen Yan, Yu Zheng, Wei Ao, Xiao Zeng, and Mi Zhang. Does unsupervised architecture representation learning help neural architecture search? *Proc. of NeurIPS*, 2020.
- [Yi *et al.*, 2023] Yun Yi, Haokui Zhang, Wenze Hu, Nannan Wang, and Xiaoyu Wang. Nar-former: Neural architecture representation learning towards holistic attributes prediction. In *Proc. of CVPR*, 2023.
- [Zhang *et al.*, 2021a] Xiong Zhang, Hongmin Xu, and Hong Mo. Dcnas: Densely connected neural architecture search for semantic image segmentation. In *Proc. of CVPR*, 2021.
- [Zhang *et al.*, 2021b] Yuge Zhang, Chenqian Yan, and Quanlu Zhang. Acenas: Learning to rank ace neural architectures with weak supervision of weight sharing. *arXiv preprint arXiv:2108.03001*, 2021.
- [Zhao *et al.*, 2023] Junbo Zhao, Xuefei Ning, Enshu Liu, and Binxin Ru. Dynamic ensemble of low-fidelity experts: Mitigating nas “cold-start”. In *Proc. of AAAI*, 2023.
- [Zheng *et al.*, 2022] Xiawu Zheng, Xiang Fei, Lei Zhang, and Chenglin Wu. Neural architecture search with representation mutual information. In *Proc. of CVPR*, 2022.
- [Zheng *et al.*, 2024] Shenghe Zheng, Hongzhi Wang, and Tianyu Mu. Dclp: Neural architecture predictor with curriculum contrastive learning. In *Proc. of AAAI*, 2024.